

# 자유곡면의 경사도에 따른 볼엔드밀링 이송속도의 최적화 연구

맹희영\*, 윤장상†

## Optimization of Ball End Milling Feedrate considering Variation of Slopes in the CNC Machining of Sculptured Surfaces

Hee-young Maeng\*, Jang-sang Yoon†

### Abstract

This study presents the analysis of ball end milling machinability and its application to the determination of the optimum feedrate in the CNC machining process of sculptured surfaces. The methods which estimate the cutting force system is approached experimentally. The estimation strategy, named technological processor, was applied to the machining process of sculptured surfaces for finding optimum variable feedrate. From the result of practical implementation for the test model, it is ascertain that the technological processor have brought the dispersion of force profiles. As compared with conventional imposing of cutting conditions, the machining time has reduced by more than 60%.

**Key Words:** *Sculptured Surfaces, Ball End Milling, Variable Feedrate, Technological Processor, Machining Time, CNC Machining.*

### 1. Introduction

The sculptured surfaces have long been machined by using the ball end mill cutters in the aerospace and die/mold industries. Most of them are recently worked on the CNC milling machines or machining centers owing to the advances in CAD/CAM technology.

As compared with other machining operations, the ball end milling process brings the fall-down of machinability that is easy to cause the chipping near the cutter tip. It is, therefore, somewhat difficult to increase the operating parameters, such

as feedrate. There have been several Japanese researches<sup>(1-5)</sup> which studied on the ball end milling ability and cutting performance for the various types of ball mill geometries. However, most of their studies are localized on the simple model testing to get the machinability data in the case of inclined milling or oblique cutting mechanism. Wang<sup>(6)</sup> attempted a solid modeling approach to optimize the metal removal rate of 3-dimensional NC end milling, and Armstrong<sup>(7)</sup> et al. have achieved the numerical code generation from a geometric modeling system.

\* 주저자, 서울산업대학교 기계설계자동화공학부 maeng@snut.ac.kr  
주소: 139-743 서울시 노원구 공릉동 172번지

† 서울산업대학교 기계설계자동화공학부

Maeng et al.<sup>(6)</sup> have studied the fundamental analysis about the cutting force system, cutter life, and economic cutting speed using the cutting parameters shown in Fig. 1 in the ball end milling of sculptured surface model. This results was used to impose the machining conditions in the rough-cut NC machining process by applying the chip load to the solid modeler or invasive machining process.

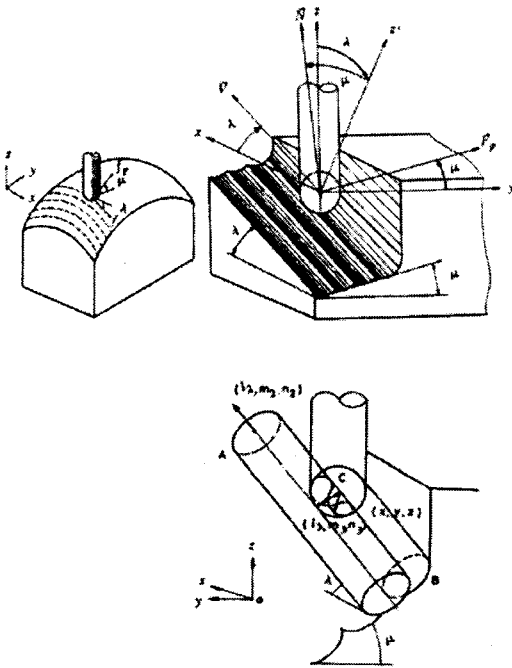


Fig. 1 Cutting parameters used to machine sculptured surfaces.

When the cutting analysis is applied to NC cutter path planning of sculptured surface, it is required a practical estimation modeler and an abundant machining data, which could be used in the real time estimation procedures. The modeler of machining for sculptured surfaces requires the geometric parameters, such as pickfeed direction and feedrate direction, in addition to the elementary operating parameters, such as the axial depth of cut and cutting width.

In order to overcome the above requirements, this study constructs the methods that estimate the cutting force system by the new approach model, and then determine the cutting speed by using the cutter life equation during the process optimization stages. Also, this approach is proved experimentally to be adequate for the practical use from an accuracy point of view and for the real time application. The technological processor, as is shown in Fig. 2, is applied to the determining the variable machining conditions during the NC path generation process of sculptured surface models.

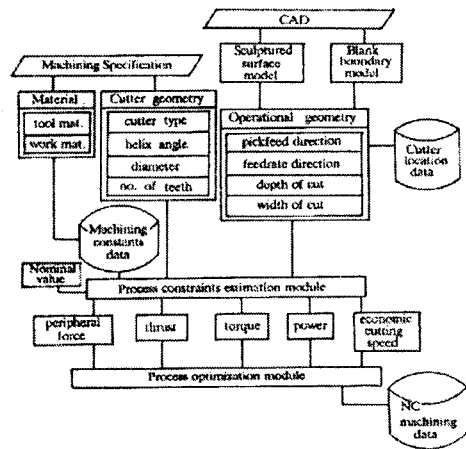


Fig. 2 Process diagram of process optimization module.

## 2. Evaluation of cutting force system

### 2.1 Average cutting force system

During the ball end milling process, the force, acting on an infinitesimal cutting edge, is made up of two components, one of which is a component proportional to the undeformed area of cut, and the other is a component proportional to the length of cutting edge engaged<sup>(5, 7)</sup> The cutting force system acting on a spiral edge could be determined by transforming the local chip load to the fixed coordinates, and then integrating along the axial

depth of cut. The average cutting force system therefore could be estimated by further integrating these components during one revolution, and by superposing for the  $m$ -pieces of cutting edge.

As a result, the average cutting force system could be expressed in down milling by defining the integrated factors as cutting action accumulating coefficients such as  $I_1, I_2, \dots, I_8^{(7)}$ , as follows

$$\begin{pmatrix} \bar{F}_x \\ \bar{F}_y \\ \bar{F}_z \\ \bar{M}_t \end{pmatrix} = m \cdot r_0 \cdot K \cdot f_i \begin{pmatrix} I_1 & I_2 & 0 \\ -I_2 & I_1 & 0 \\ 0 & 0 & I_5 \\ r_0 I_7 & 0 & 0 \end{pmatrix} \begin{pmatrix} 1 \\ r_1 \\ r_3 \end{pmatrix} \\ + m \cdot r_0 \cdot K \cdot h^* \begin{pmatrix} I_3 & I_4 & 0 \\ -I_4 & I_3 & 0 \\ 0 & 0 & I_6 \\ r_0 I_8 & 0 & 0 \end{pmatrix} \begin{pmatrix} 1 \\ r_2 \\ r_4 \end{pmatrix} \dots \dots \dots (1)$$

where  $M_t(\theta)$  is a torque, and  $\xi(\theta)$  and  $\zeta(\theta)$  is cutting existence function,  $K, r_1, r_2, r_3, r_4$  and  $h^*$  is cutting constants,  $f_i$  is feed per tooth.

### 2.2 Cutting action accumulating coefficients

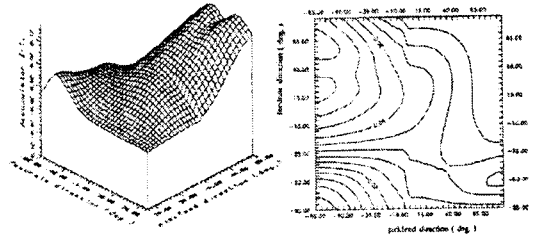
In the above equation (1), a cutting action accumulation coefficient was an integrated factors over the one revolution of cut in the cutting action region and along the helix cutting edge. For instance, in the case of  $l > r_0$ , the  $I_1$  may be integrated as follow

$$I_1 = \frac{1}{4\pi} \left[ \int_0^{\frac{\pi}{2}} 2 G_1(\delta) \cdot \sin \delta \cdot d\delta + R_k \cdot \sin^2 \phi_c \right] \quad (2)$$

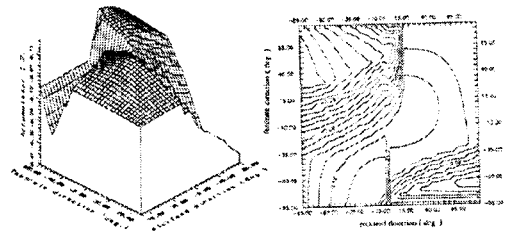
where  $G_1(\delta)$  is an integrating operator in the spherical part edge, and  $\delta$  is the location angle of infinitesimal cutting edge.

These coefficients could be calculated according to the cutting parameters such as pickfeed direction, feedrate direction, axial depth of cut, width of cut that is non-dimensionally determined by dividing the cutter radius, regardless of cutting constants<sup>(7)</sup>. When the technological estimation is processed, these coefficients may be interpolated by

the neighboring values which are searched in each stepped cutting parameter by searching the random access data-file to be pre-calculated. A variation example of cutting accumulating coefficient  $I_1$  and  $I_2$  is simulated in Fig 3.



(a) Cutting action accumulating coefficient  $I_1$



(b) Cutting action accumulating coefficient  $I_2$

Fig. 3 Variation of  $I_2$  and  $I_1$  with respect to  $\mu$  and  $\lambda$ .

### 2.3 Force concentration ratio

Compared with the chip load of cylindrical part edge, the chip load of spherical part edge acts as if it is turned over. Thus, the overall chip load configuration could be mapped into the one of flat end milling having an equivalent cutter radius. The equivalent cutter radius could be expressed as follows

$$r_0^* = \frac{\bar{M}_t}{F_T} = \frac{\bar{M}_t}{\frac{m}{2\pi} \int_0^{2\pi} dF_T \cdot d\theta} = r_0 \left\{ \frac{f_i \cdot I_7 + h^* \cdot I_8}{f_i \cdot I_4 + h^* \cdot I_6} \right\} \dots \dots \dots (3)$$

Hence the torque pattern could be superposed as the case of peripheral milling which has an equivalent cutter radius. The torque patterns have

five modes in actual ball end milling and they have a good agreement with the experimental results<sup>(7)</sup>. Therefore, the force concentration ratio in each geometrical cutting mode could be determined in terms of torque pattern models and they could be used to drive the actual peak force system.

### 3. Applicaton to CNC machining

#### 3.1 Determination of cutting parameters

Consider a cutter path moving along the curve

$$\mathbf{u} = \mathbf{u}(t) = \begin{bmatrix} u(t) \\ v(t) \end{bmatrix} \quad (6)$$

on parametric surface  $\mathbf{r} = \mathbf{r}(u, v)$  as follows

$$\mathbf{r}_c(u, v) = \mathbf{r}(u, v) + r_0 \cdot \mathbf{n} \quad (7)$$

where  $r_0$  is the cutter radius, and  $\mathbf{n}$  is the unit normal vector.

Then the four geometric cutting parameters such as  $\mu$ ,  $\lambda$ ,  $f_b$  and  $l$  could be estimated by using following relations.

First, we could express the unit tangent vector  $\mathbf{T}$  as follows

$$\mathbf{T} = \frac{\dot{\mathbf{r}}}{\|\dot{\mathbf{r}}\|} = \frac{A\dot{\mathbf{u}}}{(\mathbf{u}^T G \mathbf{u})^{1/2}} \quad (8)$$

$$\text{where } A = \begin{bmatrix} \frac{\partial \mathbf{r}}{\partial u} & \frac{\partial \mathbf{r}}{\partial v} \end{bmatrix}$$

$$\text{and } G = A^T \cdot A$$

As the y-component of  $\mathbf{T}$  is zero, it is given by

$$(\cos\lambda, 0, \sin\lambda) = (T_x^2 + T_y^2, 0, T_z) \quad (9)$$

Also the unit normal vector has the z-component as

$$n_z = \cos\mu \cdot \cos\lambda \quad (10)$$

As th pickfeed vector  $\vec{F}_P$  has the relation of

$$\vec{F}_P = f_p \cdot \frac{\mathbf{T} \times \mathbf{N}}{\|\mathbf{T} \times \mathbf{N}\|} = f_p (l_3, m_3, n_3)$$

, its z-component could be estimated as follows

$$n_3 = \sin\lambda \cdot \cos\lambda = (T_x \cdot n_y - T_y \cdot n_x) / \|\mathbf{T} \times \mathbf{N}\| \quad (11)$$

The distance of  $\Delta \mathbf{r}_2$  parallel to  $\vec{F}_P$  denoted by  $d$  is

$$d = [\Delta \mathbf{r}_2 \times \mathbf{T}] \quad (12)$$

Therefore the pickfeed, i.e. the distance  $f_p$  between the two cutter center of sphere is determined by

$$f_p = \left(1 \pm \frac{r_0}{\rho}\right) [\Delta \mathbf{r}_2 \times \mathbf{T}] \quad (13)$$

Also the axial depth of cut is determined by subtracting the z-value of cutter center location from the z-boundary value of upper blank

$$l = z_b - z + r_0 \quad (14)$$

#### 3.2 Construction of process constrains

When the sculptured surfaced is machined at the 3-axis NC milling machine, we could practically construct the following process constraints.

As a restraint of peripheral force,

$$\sqrt{1+r_1^2} \cdot R_m \cdot m \cdot r_0 \cdot K \cdot (f_t \cdot I_4 + h^* \cdot I_6) \leq F_{pc} \quad (15)$$

A restraint of thrust is given by

$$R_m \cdot m \cdot r_0 \cdot K \cdot (f_t \cdot r_3 \cdot I_5 + h^* \cdot r_4 \cdot I_6) \leq F_{tc} \quad (16)$$

and a restraint of torque is given by

$$R_m \cdot m \cdot r_0^2 \cdot K \cdot (f_t \cdot I_7 + h^* \cdot I_8) \leq M_{tc} \quad (17)$$

and maximum feedrate is restricted by

$$m \cdot f_t \cdot n \leq f_{mc} \text{ (mm/min.)} \quad (18)$$

Therefore these constrains could be satisfied by following procedure.

(a) STEP I : Search for  $f_t$  given by

$$\text{MIN} (f_{t15}, f_{t16}, f_{t17})$$

(b) STEP II : Calculate the spindle speed  $n_{18}$

(c) STEP III : Calculate the feedrate

$$f_m = m \cdot f_t \cdot n$$

#### 3.3 Implementation to the processor

We have called the 'technological processor' as the procedure that determine the optimum cutting

conditions by processing the previous 3 steps. This procedure should be performed at each segment of cutter path and be executed in a real time for the practical use. Because the estimation algorithms are used by simple search process, we could fortunately execute this procedure within real time.

#### 4. Case study

This technological processor is applied to the test sculptured surface model that is composed with the form of explicit function as follows

$$z = f(x, y) = 40xy(x^2 - y^2)/(x^2 + y^2 + 0.25)$$

as is shown in Fig. 4. The shape of blank is cube form that has a size of  $120 \times 80 \times 50$  mm, and inner tolerance is 0 mm, and cusp height is 0.2 mm. Also the cutter path is determined using the pendulum mode path so that down milling always should be applied. Fig. 5(a) and (b) show the simulation of operational geometry and Fig. 6 is the resultant variable cutting condition applied to the machining of aluminium alloy(3003H12) workpiece. In this example, total length of cutter path is 5385.6 mm. The total machining time has been required 31.3 minutes for carbon steel(SM45C) workpiece. If the skillful technician works on the machining of this aluminum alloy workpiece with the feedrate of 80 mm/min, it requires 79.8 minutes, and in the case of carbon steel workpiece, it requires 147 minutes with the feedrate of 40mm/min.

Therefore the total machining times is saved 60.7 % for aluminium alloy workpiece and 62.7 % for carbon steel workpiece. Fig. 7 is the comparison of cutting force profiles between constant feed and variable feed machining with a cutter path. This indicates that variable feed machining exhibits the force dispersion and full use of the machine tool capability effectively.

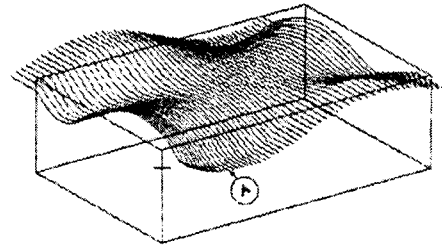
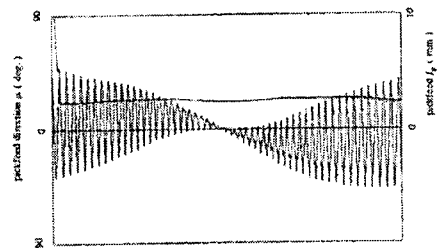
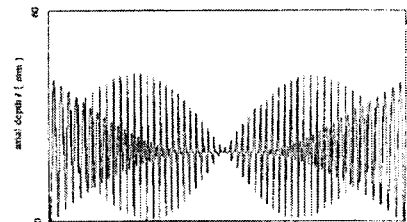


Fig. 4 View and cutter path of a test sculptured surface model.



(a) Simulation of  $\mu$  and  $f_p$



(b) Simulation of axial depth  $l$

Fig. 5 Simulation of operational geometric parameters.

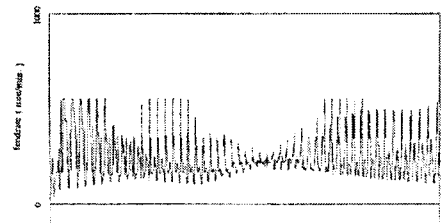
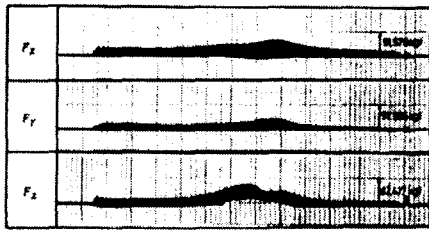
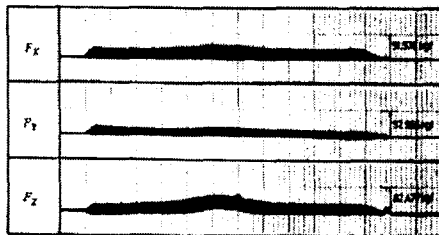


Fig. 6 Variable feedrate resulted from technological process optimization.



(a) constant feedrate



(b) variable feedrate

Fig. 7 Comparison of cutting force profiles between constant and variable feedrate.

## 5. Conclusions

Through the technological estimation analysis about the ball end milling system, the practical expressions could be applied in this study to the NC machining of sculptured surfaces in the optimization process of operating parameters.

It has been defined the cutting action accumulating coefficients, force concentration ratios, and economic cutting speed equation, which could be evaluated as the function of geometrical parameters regardless of cutting constants. And then, these factors were prepared for the practical use as the random access files after being calculated in advance for the each stepped cutting parameters. Therefore, the process constraints could be estimated within a real time and within a proper accuracy.

The technological processor has been used to find the variable cutting conditions in each segment

of cutter path for the test sculptured surface models. It is finally recognized that variable machining conditions have made an effect on the saving of total machining time over 60% and have resulted the dispersion of cutting force profiles remarkably than the conventional determination of cutting conditions.

## Reference

- (1) Kishinami, "On Relationship between Cutting Ability and Cutting Edge Shape of CCE Ball End Mill", J. of JSPE, Vol. 48, No. 7, pp. 68~74, 1982.
- (2) Aoyama, H., et al., "Study on Development and Cutting Performance of Elliptic Ball End Mill", J. of JSPE, Vol. 53, No. 3, pp. 461~466, 1987.
- (3) Hosoi, T. et al., "Cutting Actions of Ball End Mill With a Spiral Edge", Annals of the CIRP, Vol. 25, No. 1, 1987.
- (4) Fujii and Iwabe, "Relationship between Cutting Force Curve and Working Accuracy with Ball-nose End Mills", J. of JSPE, Vol. 48, pp. 105~110, 1982.
- (5) Miyazawa and Takeda, "Micro milling of Three Dim. Surface", J. of JSPE, Vol. 47, pp. 94~99, 1981.
- (6) Wang, W.P., "Solid Modeling for Optimizing Metal Removal of Three-Dimensional NC End Milling", J. of Manufacturing Systems, Vol. 15, No. 1, 1996.
- (7) Armstrong, G. T. et al., "Numerical Code Generation from a Geometric Modeling System", Solid Modeling by computers, Plenum press, N.Y., pp. 139~157, 1997.
- (8) Park, C. and Maeng, H., "A Study on Cutting Force System of Conical Tipped Ball End Mill", J. of KSME, Vol. 9, No. 4, 1985.
- (9) Ber A., Rotberg, J. and Zombach, S., "A Method of Cutting Force Evaluation of End Mills", Annals of the CIRP, Vol.42, No. 1, 1993.
- (10) Yellowley, I., "Observations on the Mean Values of Forces, Torque and Specific Power in the Peripheral Milling Process", Int. J. of MDR, Vol. 25, No. 4, pp. 337~346, 1985.